

The chiral magnetic effect in heavy-ion collisions from event-by-event anomalous hydrodynamics

Yuji Hirono,^{1,*} Tetsufumi Hirano,² and Dmitri E. Kharzeev^{1,3}

¹ *Department of Physics and Astronomy, Stony Brook University, Stony Brook, New York 11794-3800, USA*

² *Department of Physics, Sophia University, Tokyo 102-8554, Japan*

³ *Department of Physics, Brookhaven National Laboratory, Upton, New York 11973-5000, USA*

(Dated: August 30, 2015)

The (3+1)D relativistic hydrodynamics with chiral anomaly is used to obtain a quantitative description of the chiral magnetic effect (CME) in heavy-ion collisions. We find that the charge-dependent hadron azimuthal correlations are sensitive to the CME, and that the experimental observations are consistent with the presence of the effect.

PACS numbers:

The experimental study of charge-dependent hadron azimuthal correlations in heavy-ion collisions at RHIC [1, 2] and LHC [3] revealed a signal qualitatively consistent with the separation of electric charge predicted [4] as a signature of local \mathcal{P} - and \mathcal{CP} -odd fluctuations in QCD matter. The subsequent studies [5–7] improved the theoretical understanding of the underlying phenomenon – the separation of electric charge in the quark-gluon plasma induced by the chirality imbalance in the presence of background magnetic field, or the “chiral magnetic effect” (CME), see Ref. [8] for a review and additional references. The existence of CME has been confirmed in first-principle lattice QCD×QED simulations [9–12]. By holographic methods, the CME has also been found to persist at strong coupling [13], in accord with its non-dissipative, topologically protected nature.

Because the macroscopic behavior of matter at strong coupling is described by hydrodynamics, it is natural to address the question of the existence of CME within the framework of fluid dynamics. Son and Surowka [14] showed that the CME indeed is an integral part of relativistic hydrodynamics, and moreover its strength as fixed by the second law of thermodynamics is consistent with the field-theoretical prediction. The CME current in the hydrodynamic regime is carried by a novel collective gapless excitation, the chiral magnetic wave [15, 16]. Conformal anomalous hydrodynamics at second order in the derivative expansion has been formulated in [17].

Relativistic hydrodynamics with fluctuating initial conditions proved very successful in explaining the bulk of RHIC and LHC data (see Refs. [18–20] for recent reviews). It is thus appropriate to rely on this approach also for describing the CME in heavy-ion collisions, by using hydrodynamics with the terms induced by chiral anomaly and magnetic fields – so-called anomalous hydrodynamics, or chiral magnetohydrodynamics (CMHD). The first pilot numerical study of anomalous hydrodynamics was performed in Ref. [21], where the effects of anomaly on the charge-dependent elliptic flow were investigated. Nevertheless, a fully quantitative description of the experimental data on charge-dependent

azimuthal correlations has not been performed until now. In this Letter, we perform such a study basing on three-dimensional ideal CMHD with event-by-event fluctuations in the initial conditions.

Let us first describe the measured experimental observable [22] sensitive to the CME that we aim to describe. The azimuthal-angle distribution of observed particles reads

$$\frac{dN^\alpha}{d\phi} \propto 1 + 2v_1^\alpha \cos(\phi - \Psi_{\text{RP}}) + 2a_1^\alpha \sin(\phi - \Psi_{\text{RP}}) + \sum_{n>1} 2v_n^\alpha \cos n(\phi - \Psi_n), \quad (1)$$

where $\alpha \in \{+, -\}$. The Fourier coefficients v_n^\pm of the azimuthal-angle distribution characterize the shape of the produced matter in momentum space. The component with $n = 1$ is called the directed flow. In Eq. (1), we decomposed the directed flow into two directions, along

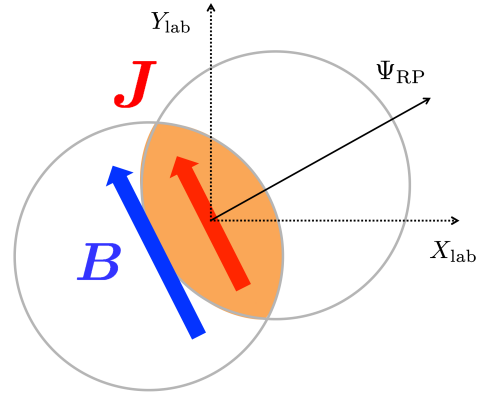


FIG. 1: Schematic picture of a heavy-ion collision event in the transverse plane. \mathbf{B} indicates the magnetic field, and \mathbf{J} is the electric current induced by the chiral magnetic effect in the case of a positive initial axial charge density. The direction of \mathbf{J} is flipped if the initial axial charge is negative.

(v_1^α) and perpendicular to (a_1^α) the reaction plane angle Ψ_{RP} (see Fig. 1).

The coefficients a_1^\pm are expected to exhibit the presence of CME [4, 22]. Indeed, suppose that a heavy-ion collision creates a localized lump of a positive axial charge. Because of the presence of the out-of-plane magnetic field [6], the CME current is generated in the direction of the magnetic field, leading to the formation of a charge dipole. The collective expansion of matter translates this dipole into the charge-dependent flow quantified by a_1^\pm . For a positive initial axial charge, $a_1^+ > 0$ and $a_1^- < 0$, since positive particles tend to move along the direction of magnetic field and negative particles move in the opposite direction. In contrast, if the initial axial charge is negative, the result is $a_1^+ < 0$ and $a_1^- > 0$ since the direction of the electric current is reversed. The coefficients a_1^\pm can thus indeed be affected by the CME.

However, a_1^\pm in a single event is very sensitive to statistical fluctuations – we are thus forced to study the quantities averaged over many events. Since there is no preferred sign of the initial axial charge, the event averages of a_1^\pm vanish, $\langle a_1^+ \rangle = \langle a_1^- \rangle = 0$. We thus have to look at the fluctuations of a_1^\pm . The CME-based expectations for these quantities are the following:

1. The fluctuation $\langle (a_1^\pm)^2 \rangle$ would become larger in the presence of anomalous transport effects.
2. There would be an anti-correlation between a_1^+ and a_1^- , so that $\langle a_1^+ a_1^- \rangle < 0$.

To quantify the strength of \mathcal{P} -odd fluctuations, the following observable has been proposed [22] and measured by the STAR Collaboration [2]:

$$\gamma_{\alpha\beta} \equiv \langle \cos(\phi_1^\alpha + \phi_2^\beta - 2\Psi_{\text{RP}}) \rangle, \quad (2)$$

where ϕ_1^α and ϕ_2^β are the azimuthal angles of the first and second particle, and $\alpha, \beta \in \{+, -\}$ indicate their charges. The physical meaning of the observable (2) becomes evident if we re-write ($\Delta\phi^\alpha \equiv \phi^\alpha - \Psi_{\text{RP}}$)

$$\begin{aligned} \langle \cos(\phi_1^\alpha + \phi_2^\beta - 2\Psi_{\text{RP}}) \rangle &= \langle \cos \Delta\phi_1^\alpha \cos \Delta\phi_2^\beta \rangle \\ &- \langle \sin \Delta\phi_1^\alpha \sin \Delta\phi_2^\beta \rangle \equiv \langle v_1^\alpha v_1^\beta \rangle - \langle a_1^\alpha a_1^\beta \rangle. \end{aligned} \quad (3)$$

One can see that γ_{++} and γ_{--} are sensitive to $\langle (a_1^\pm)^2 \rangle$, and γ_{+-} to $\langle a_1^+ a_1^- \rangle$. Another merit of using (3) is that the reaction-plane-independent background effects are eliminated by the subtraction between $\langle (v_1)^2 \rangle$ and $\langle (a_1)^2 \rangle$ [2].

The equations of motion of anomalous hydrodynamics are given by

$$\partial_\mu T^{\mu\nu} = eF^{\nu\lambda} j_\lambda, \quad (4)$$

$$\partial_\mu j^\mu = 0, \quad (5)$$

$$\partial_\mu j_5^\mu = -CE_\mu B^\mu, \quad (6)$$

where $C \equiv \frac{N_c}{2\pi^2} \sum_f q_f^2$ is the anomaly constant, $E^\mu \equiv F^{\mu\nu} u_\nu$, $B^\mu \equiv \tilde{F}^{\mu\nu} u_\nu$ with $\tilde{F}^{\mu\nu} = \frac{1}{2}\epsilon^{\mu\nu\alpha\beta} F_{\alpha\beta}$. In this

study, the electromagnetic fields are treated as background fields. We consider three light flavors of quarks and for simplicity put their electric charges $q_f = 1$; introducing real charges of quarks would amount to a simple rescaling of charge densities in the equations below. The fluid is assumed to be dissipationless (note that the CME current is non-dissipative), so the energy-momentum tensor, the electric and axial currents are written as

$$T^{\mu\nu} = (\varepsilon + p)u^\mu u^\nu - p\eta^{\mu\nu}, \quad (7)$$

$$j^\mu = nu^\mu + \kappa_B B^\mu, \quad (8)$$

$$j_5^\mu = n_5 u^\mu + \xi_B B^\mu, \quad (9)$$

where ε is the energy density, p is the hydrodynamic pressure, n and n_5 are electric and axial charge densities, $e\kappa_B \equiv C\mu_5(1 - \mu_5 n_5/(\varepsilon + p))$ and $e\xi_B \equiv C\mu(1 - \mu n/(\varepsilon + p))$ are transport coefficients, and $\eta^{\mu\nu} \equiv \text{diag}\{1, -1, -1, -1\}$ is the Minkowski metric. The second terms in Eq. (8) and Eq. (9) correspond to the chiral magnetic effect and the chiral separation effect, respectively. The values of κ_B and ξ_B are determined by requiring that the entropy does not decrease [14], or from the condition of zero entropy production from anomalous currents [17], with an equivalent result.

Hydrodynamic equations should be augmented with an equation of state (EOS). Here we use EOS of a massless ideal quark-gluon gas [37], $\varepsilon = 3p$, with

$$\begin{aligned} p(T, \mu, \mu_5) &= \frac{g_{\text{QGP}}\pi^2}{90} T^4 + \frac{N_c N_f}{6} (\mu^2 + \mu_5^2) T^2 \\ &+ \frac{N_c N_f}{12\pi^2} (\mu^4 + 6\mu^2 \mu_5^2 + \mu_5^4), \end{aligned} \quad (10)$$

where $g_{\text{QGP}} = g_g + \frac{7}{8}g_q$ is the number of degrees of freedom with $g_g = (N_c^2 - 1)N_s$ and $g_q = 2N_c N_s N_f$; $N_c = 3$ and $N_f = 3$ are the numbers of colors and flavors and $N_s = 2$ is the number of spin states for quarks and (transverse) gluons. The entropy, electric, and axial charge densities are obtained from Eq. (10) as $s = \frac{\partial p}{\partial T}$, $n = \frac{\partial p}{\partial \mu}$, and $n_5 = \frac{\partial p}{\partial \mu_5}$.

In order to switch from hydrodynamic degrees of freedom to individual particles, we use the standard Cooper-Frye approach [23], on an isothermal freezeout hypersurface with $T_{\text{fo}} = 160$ MeV. We perform Monte-Carlo samplings of hadrons on the freezeout surface following the procedure described in detail in Ref. [18].

As a background electromagnetic field, we take B_y to be (x -axis is taken to be Ψ_{RP})

$$eB_y(\tau, \eta_s, \mathbf{x}_\perp) = eB_0 \frac{b}{2R} \exp \left[-\frac{x^2}{\sigma_x^2} - \frac{y^2}{\sigma_y^2} - \frac{\eta_s^2}{\sigma_{\eta_s}^2} - \frac{\tau}{\tau_B} \right], \quad (11)$$

where σ_x , σ_y , and σ_{η_s} are the widths of the field in x , y , and η_s (space-time rapidity) directions, τ_B is the decay time of the magnetic field, $R = 6.38$ fm is the radius of a gold nucleus, and b is the impact parameter. Other components of \mathbf{B} and \mathbf{E} were set to zero.

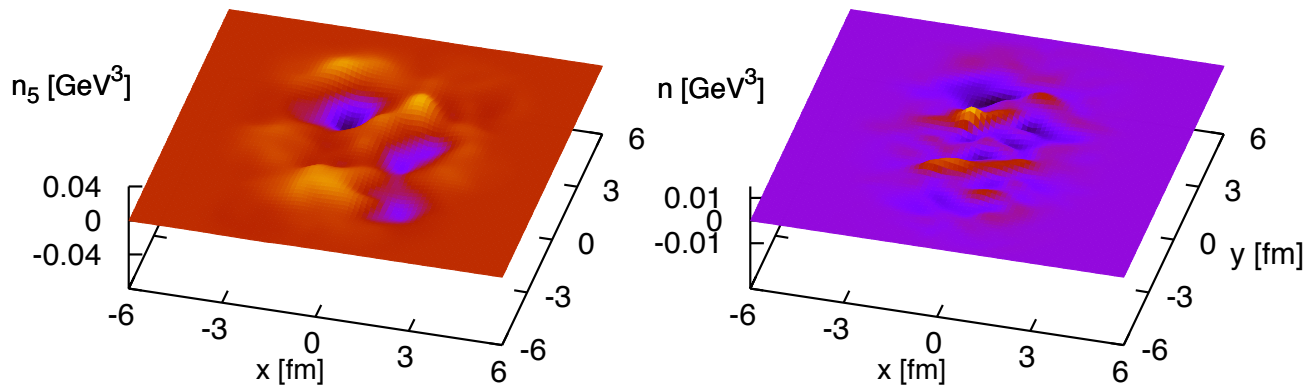


FIG. 2: Axial charge (left) and electric charge (right) densities at $\tau = 1.5$ fm in the transverse plane ($\eta_s = 0$).

We assume the strength of the magnetic field (11) to be proportional to the impact parameter [6]. The widths are chosen as $\sigma_x = 0.8(R - \frac{b}{2})$, $\sigma_y = 0.8\sqrt{R^2 - (b/2)^2}$, and $\sigma_\eta = \sqrt{2}$, so that the fields are applied only in the region where matter exists. We set $\tau_B = 3$ fm and $eB_0 = 0.5\text{GeV}^2$ for the following calculations, which corresponds to $eB_y(\tau_{\text{in}}, 0, \mathbf{0}) \sim (3m_\pi)^2$.

For the modeling of the initial axial charge density, we make an extension to the Monte-Carlo (MC) Glauber model [24]. We assume that the initial axial charge density is generated by the color flux tubes during the early moments of the heavy-ion collision [25, 26]. In this picture, the parallel chromo-electric \mathbf{E}^a and chromo-magnetic \mathbf{B}^a fields (with strength $\sim Q_s^2/g$ determined by the saturation momentum Q_s) create the axial charge through the chiral anomaly equation $\partial_\mu j_5^\mu = \frac{g^2}{16\pi^2} \mathbf{E}^a \cdot \mathbf{B}^a$. First, we assign ± 1 for each binary collision randomly – each sign corresponds to the sign of $\mathbf{E}^a \cdot \mathbf{B}^a$ for a color flux tube where the color orientations of \mathbf{E}^a and \mathbf{B}^a change after each collision due to the color exchanges. Then, when we calculate the axial chemical potential for a particular point in the transverse plane, we sum the signs over the collisions occurring at that position and multiply it by a dimensionful constant C_{μ_5} .

We estimate the parameter C_{μ_5} as follows. Integrating the chiral anomaly equation, we find the axial charge density at the time τ_{in} at which the hydrodynamic evolution is initialized:

$$n_5(\tau_{\text{in}}) \sim \tau_{\text{in}} \times \frac{g^2}{16\pi^2} \mathbf{E}^a \cdot \mathbf{B}^a. \quad (12)$$

We take $\tau_{\text{in}} \sim 0.6$ fm $\simeq 3$ GeV $^{-1}$, and estimate the strength of the gluon fields from the saturation scale at RHIC as $g|\mathbf{E}^a| \sim g|\mathbf{B}^a| \sim 1$ GeV 2 [27, 28] $n_5(\tau_{\text{in}}) \sim$

$(0.4 \text{ GeV})^3$, translating into μ_5 is of the order of 0.1 GeV; we thus set the coefficient $C_{\mu_5} = 0.1$ GeV. From the values of $\mu_5(\mathbf{x}_T, \eta_s)$ and the entropy $s(\mathbf{x}_T, \eta_s)$, we determine the initial T . The initial flow velocity and electric charge density are taken to be zero [38].

We first generate an initial condition by the MC-Glauber model including the effect of fluctuating axial charge densities, at a fixed impact parameter. Then we let the matter evolve according to anomalous hydrodynamic equations, getting a freezeout hypersurface. Sampling particles from the surface, we get the data for an event. We repeat this process to accumulate the data for many events. We performed the simulations for three impact parameters, $b = 7.2, 9.0, 11.2$ fm (20-30%, 30-40%, 50-60% in centrality). For each impact parameter, we calculated 100k, 150k, and 250k events for both of anomalous and non-anomalous cases. In the “non-anomalous” case, the anomaly constant is set to zero and there is no CME.

Let us first look at how the charge profile is affected by the anomalous transport. Figure 2 shows the axial charge density and electric charge densities in the transverse plane ($\eta_s = 0$) for an event. As is evident from the right figure, the CME leads to a non-trivial electric charge profile. (If we switch off the anomalous transport effect, the electric charge density is zero throughout the evolution.) One can see a number of charge dipoles formed in areas where there was a non-zero axial charge. The direction of a dipole is determined by the sign of the axial charge of density.

Next, let us turn to the charge-dependent correlation functions. The correlations $\gamma_{++}(\gamma_{--})$ and γ_{+-} are cal-

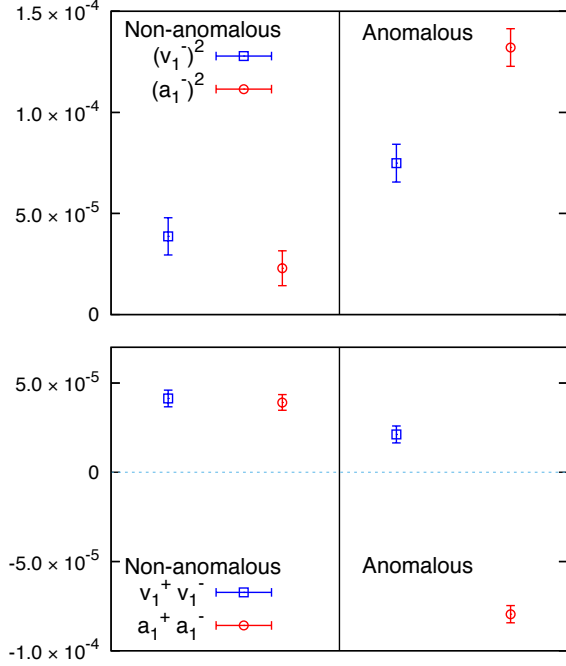


FIG. 3: $\langle (v_1^-)^2 \rangle$, $\langle (a_1^-)^2 \rangle$ (upper figure), $\langle v_1^+ v_1^- \rangle$, and $\langle a_1^+ a_1^- \rangle$ (lower figure) for anomalous and non-anomalous cases at $b = 7.2$ fm (20-30% in centrality).

culated via

$$\gamma_{\alpha\alpha} \equiv \left\langle \frac{1}{M_\alpha P_2} \sum_{\langle i,j \rangle \in S_\alpha} \cos(\phi_i + \phi_j - 2\Psi_{\text{RP}}) \right\rangle, \quad (13)$$

$$\gamma_{\alpha\beta} \equiv \left\langle \frac{1}{M_\alpha M_\beta} \sum_{i \in S_\alpha} \sum_{j \in S_\beta} \cos(\phi_i + \phi_j - 2\Psi_{\text{RP}}) \right\rangle, \quad (14)$$

where $\alpha \neq \beta$, S_α is the set of particles with charge α , $\langle i,j \rangle \in S$ in the summation symbol indicate the pair of particles in a particle set S , and the overall $\langle \dots \rangle$ means the event average. Similarly, we separately evaluate $\langle (v_1^\alpha)^2 \rangle$ and $\langle (a_1^\alpha)^2 \rangle$ by

$$\langle (v_1^\alpha)^2 \rangle \equiv \left\langle \frac{1}{M_\alpha P_2} \sum_{\langle i,j \rangle \in S_\alpha} \cos \Delta\phi_i^\alpha \cos \Delta\phi_j^\alpha \right\rangle, \quad (15)$$

$$\langle (a_1^\alpha)^2 \rangle \equiv \left\langle \frac{1}{M_\alpha P_2} \sum_{\langle i,j \rangle \in S_\alpha} \sin \Delta\phi_i^\alpha \sin \Delta\phi_j^\alpha \right\rangle. \quad (16)$$

Upper figure of Fig. 3 shows $\langle (v_1^-)^2 \rangle$ and $\langle (a_1^-)^2 \rangle$ in anomalous and non-anomalous cases at $b = 7.2$ fm (20-30% in centrality). As shown in the figure, the fluctuation of v_1 becomes large in the presence of CME, and the fluctuation of a_1 becomes even larger. The observable γ_{--} is the difference between v_1 and a_1 fluctuations, so it becomes negative, which is consistent with the experiment. The magnitude of γ_{--} is also comparable to the

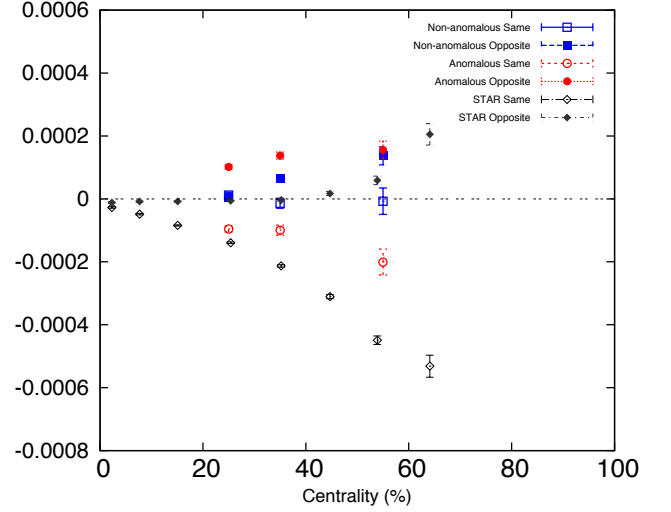


FIG. 4: Centrality dependence of γ_{++} and γ_{+-} as well as the experimental data from STAR [2].

values measured in STAR. The large value of $\langle a_1^2 \rangle$ is in line with the expectation from the CME.

In the lower figure of Fig. 3, we show the values of $\langle v_1^+ v_1^- \rangle$ and $\langle a_1^+ a_1^- \rangle$. When there is no anomalous transport, the values for $\langle v_1^+ v_1^- \rangle$ and $\langle a_1^+ a_1^- \rangle$ are positive and comparable. When anomalous transport effects are turned on, $\langle a_1^+ a_1^- \rangle$ takes a negative value. This means the anti-correlation between a_1^+ and a_1^- , which is expected from the CME.

In Fig. 4, the centrality dependence of the observables γ_{++} and γ_{+-} as well as the experimental values from STAR [29] are plotted. The values of the same-charge combination γ_{++} are negative and the magnitude increases as a function of centrality in the anomalous case, while the values are consistent with zero in the non-anomalous case. As for the opposite charge combination γ_{+-} , the values are positive and are larger in peripheral collisions in the anomalous case. The positiveness comes from negative values of $\langle a_1^+ a_1^- \rangle$, which indicates the anti-correlation between a_1^+ and a_1^- . At two peripheral centralities, γ_{+-} is positive even for the non-anomalous case.

Let us comment on the implications of this work to the possible background effects discussed in the literature. It has been pointed out that the observed values of $\gamma_{\alpha\beta}$ may be reproduced by other effects unrelated to anomalous transport, including transverse momentum conservation and flow [30, 31], charge conservation and flow [32], or cluster particle correlations [33]. All of these background effects originate from multi-particle correlations. Since neither local charge conservation nor transverse momentum conservation are imposed in our current sampling procedure, the computed correlators do not originate from these multi-particle correlations - therefore, we expect the measured correlators to reflect the presence of

CME, even though of course we cannot exclude the possible contributions from backgrounds.

We believe that event-by-event anomalous hydrodynamics is an appropriate tool for the quantitative test of the CME in heavy-ion collisions. However, it is still in the early stage and there is a lot of room for improvement in the current model. Possible future improvements include: *i*) event-by-event fluctuations of magnetic fields [34, 35]; *ii*) refinement of the modeling of initial axial charge density, possibly based on the numerical solution of Yang-Mills equations; *iii*) dynamical electromagnetic fields; *iv*) dissipative effects, including shear and bulk viscosities, Ohmic conductivity, etc. In parallel with those improvements of the model, we plan to perform a more detailed analysis of $\gamma_{\alpha\beta}$, including the dependence on transverse momentum, rapidity, collision energy and the nuclear species.

To summarize, we have performed a quantitative study of charge-dependent azimuthal hadron correlations in heavy-ion collisions using anomalous relativistic hydrodynamics. Our results indicate that these correlations are sensitive to the chiral magnetic effect, and that the pattern and the magnitude of measured correlations are in accord with anomalous hydrodynamics – even though the theoretical uncertainties are still substantial.

The authors are grateful to M. Hongo, K. Murase, S. Schlichting, Y. Tachibana, and Y. Yin for useful discussions. This work was supported in part by the U.S. Department of Energy under Contracts No. DE-FG-88ER40388 and DE-AC02-98CH10886. Y. H. is supported by JSPS Research Fellowships for Young Scientists. The work of T. H. was supported by JSPS KAKENHI Grants No. 25400269.

* Electronic address: yuji.hirono@stonybrook.edu

- [1] B. Abelev et al. (STAR Collaboration), Phys.Rev.Lett. **103**, 251601 (2009), 0909.1739.
- [2] B. Abelev et al. (STAR Collaboration), Phys.Rev. **C81**, 054908 (2010), 0909.1717.
- [3] B. Abelev et al. (ALICE Collaboration), Phys.Rev.Lett. **110**, 012301 (2013), 1207.0900.
- [4] D. Kharzeev, Phys.Lett. **B633**, 260 (2006), hep-ph/0406125.
- [5] D. Kharzeev and A. Zhitnitsky, Nucl.Phys. **A797**, 67 (2007), 0706.1026.
- [6] D. E. Kharzeev, L. D. McLerran, and H. J. Warringa, Nucl.Phys. **A803**, 227 (2008), 0711.0950.
- [7] K. Fukushima, D. E. Kharzeev, and H. J. Warringa, Phys.Rev. **D78**, 074033 (2008), 0808.3382.
- [8] D. E. Kharzeev, Prog.Part.Nucl.Phys. **75**, 133 (2014), 1312.3348.
- [9] P. Buividovich, M. Chernodub, E. Luschevskaya, and M. Polikarpov, Phys.Rev. **D80**, 054503 (2009), 0907.0494.
- [10] M. Abramczyk, T. Blum, G. Petropoulos, and R. Zhou, PoS **LAT2009**, 181 (2009), 0911.1348.
- [11] A. Yamamoto, Phys.Rev.Lett. **107**, 031601 (2011), 1105.0385.
- [12] G. Bali, F. Bruckmann, G. Endrödi, Z. Fodor, S. Katz, et al., JHEP **1404**, 129 (2014), 1401.4141.
- [13] H.-U. Yee, JHEP **0911**, 085 (2009), 0908.4189.
- [14] D. T. Son and P. Surowka, Phys.Rev.Lett. **103**, 191601 (2009), 0906.5044.
- [15] D. E. Kharzeev and H.-U. Yee, Phys.Rev. **D83**, 085007 (2011), 1012.6026.
- [16] Y. Burnier, D. E. Kharzeev, J. Liao, and H.-U. Yee, Phys.Rev.Lett. **107**, 052303 (2011), 1103.1307.
- [17] D. E. Kharzeev and H.-U. Yee, Phys.Rev. **D84**, 045025 (2011), 1105.6360.
- [18] T. Hirano, P. Huovinen, K. Murase, and Y. Nara, Prog.Part.Nucl.Phys. **70**, 108 (2013), 1204.5814.
- [19] U. Heinz and R. Snellings, Ann.Rev.Nucl.Part.Sci. **63**, 123 (2013), 1301.2826.
- [20] H. Petersen, J.Phys. **G41**, 124005 (2014), 1404.1763.
- [21] M. Hongo, Y. Hirono, and T. Hirano (2013), 1309.2823.
- [22] S. A. Voloshin, Phys.Rev. **C70**, 057901 (2004), hep-ph/0406311.
- [23] F. Cooper and G. Frye, Phys.Rev. **D10**, 186 (1974).
- [24] B. Alver, M. Baker, C. Loizides, and P. Steinberg (2008), 0805.4411.
- [25] D. Kharzeev, A. Krasnitz, and R. Venugopalan, Phys.Lett. **B545**, 298 (2002), hep-ph/0109253.
- [26] T. Lappi and L. McLerran, Nucl.Phys. **A772**, 200 (2006), hep-ph/0602189.
- [27] D. Kharzeev and M. Nardi, Phys.Lett. **B507**, 121 (2001), nucl-th/0012025.
- [28] D. Kharzeev and E. Levin, Phys.Lett. **B523**, 79 (2001), nucl-th/0108006.
- [29] L. Adamczyk et al. (STAR Collaboration) (2013), 1302.3802.
- [30] A. Bzdak, V. Koch, and J. Liao, Phys.Rev. **C83**, 014905 (2011), 1008.4919.
- [31] S. Pratt (2010), 1002.1758.
- [32] S. Schlichting and S. Pratt (2010), 1005.5341.
- [33] F. Wang, Phys.Rev. **C81**, 064902 (2010), 0911.1482.
- [34] A. Bzdak and V. Skokov, Phys.Lett. **B710**, 171 (2012), 1111.1949.
- [35] J. Błoczyński, X.-G. Huang, X. Zhang, and J. Liao, Phys.Lett. **B718**, 1529 (2013), 1209.6594.
- [36] K. Fukushima, D. E. Kharzeev, and H. J. Warringa, Phys.Rev.Lett. **104**, 212001 (2010), 1002.2495.
- [37] In hydrodynamic models, it is now standard to use an EOS calculated from lattice QCD. In the present calculations, we need μ and μ_5 dependence, which is not yet available from the lattice – so here we use the EOS of an ideal gas.
- [38] Charge separation can also occur before the onset of hydrodynamic evolution. Here, by taking $n(\tau_{in}, \eta_s, \mathbf{x}_T) = 0$, we are focusing on the charge separation in the hydro phase. The charge separation in the non-equilibrium gluonic matter is discussed in [36].